*e-X*tra*

A Partial Chromosomal Deletion Caused by Random Plasmid Integration Resulted in a Reduced Virulence Phenotype in *Fusarium graminearum*

Thomas K. Baldwin,[1] Iffa Gaffoor,[2] John Antoniw,[1] Corrie Andries,[2] John Guenther,[2] Martin Urban,[1] Heather E. Hallen-Adams,[2] John Pitkin,[3] Kim E. Hammond-Kosack,[1] and Frances Trail[2]

[1]Department of Plant Pathology and Microbiology, Rothamsted Research, Harpenden, Herts, AL5 2JQ, U.K.; [2]Departments of Plant Biology and Plant Pathology, Michigan State University, East Lansing, MI 48824, U.S.A.; [3]Monsanto Co., 700 Chesterfield Pkwy W, Chesterfield, MO 63017-1732, U.S.A.

Fusarium graminearum (teleomorph: *Gibberella zeae*) is an Ascomycete fungal plant pathogen which infects a range of agriculturally important crops, including wheat, barley, and maize. A random plasmid insertion mutagenesis approach was used to analyze the pathogenicity of the PH-1 strain, for which full genomic information is available. Fungal transformants were initially screened for their ability to infect wheat ears. From a total of 1,170 transformants screened, eight were confirmed to be highly reduced in pathogenicity toward wheat ears and roots. These were designated disease-attenuated *F. graminearum* (*daf*) mutants. The in vitro growth rate and appearance of each *daf* mutant was equivalent to the parental strain. Deoxynivalenol (DON) was not detected in threshed grain recovered from ears inoculated with the *daf10* mutant. Plasmid rescue and sequencing of the mutant *daf10* revealed a deletion of approximately 350 kb from one end of chromosome 1. This chromosome segment is predicted to contain 146 genes. Microarray analysis of *daf10* gene expression during growth in DON-inducing conditions confirmed the large deletion. The identities of the genes deleted and their potential role in DON production, pathogenesis, and other life processes are discussed.

Fusarium ear blight (FEB) disease of cereal crops causes considerable losses in grain quality and safety throughout the world (Parry et al. 1995; Beacham et al. 2009; Trail 2009). The two main pathogens which cause FEB on wheat are the fungi

Fusarium graminearum Schwabe, sexual stage *Gibberella zeae* (Schwein.) Petch, and *F. culmorum* (W. G. Sm.) Sacc.

F. graminearum and *F. culmorum* produce a range of B-type trichothecene compounds, including nivalenol (NIV), deoxynivalenol (DON, also known as vomitoxin), and the acetylated derivatives 3-acetyl-DON and 15-acetyl-DON. These are sesquiterpenoid toxins produced as secondary metabolites which accumulate in the infected grain of wheat (Kimura et al. 2007). Consumption of trichothecene compounds can cause health problems in animals, poultry, and humans. In addition, FEB is associated with a reduction in the baking and brewing qualities of infected grain. Legislation now limits DON concentrations in finished grain products for human consumption to 1 ppm in the United States and 0.5 ppm in the European Union (European Commission Regulation no. 856/2005).

In *F. graminearum* and the related *Fusarium* sp., *F. sporotrichioides*, the biosynthetic pathway for trichothecene mycotoxins has been intensively investigated. The genes for DON biosynthesis reside primarily in a 25-kb cluster, a second, smaller two-gene cluster, and at least one gene, *TRI101*, residing elsewhere (Kimura et al. 2007). The major cluster includes *TRI5*, encoding trichodiene synthase, which is responsible for generation of trichodiene from farnesyl pyrophosphate, and structural genes *TRI3–TRI114*. *TRI1*, a regulatory gene, and *TRI16* reside elsewhere in the genome. *TRI4*, *TRI101, TRI11*, and *TRI3* catalyze the synthesis of calonectrin, which can then be used to synthesize nivalenol, 3-acetyl-DON, 15-acetyl-DON, or DON, in *F. graminearum*, or as a precursor to T-2 toxin in other fungi. Biosynthesis of 15-acetyl-DON and DON requires the presence of the *TRI8* and *TRI1* genes for completion of the pathway. *TRI6* and *TRI10* are regulatory genes (Seong et al. 2009). The generation of *F. graminearum* mutants unable to produce DON, by targeted gene deletion, has revealed the importance of this mycotoxin during the infection of wheat ears (Proctor et al. 1995; Jansen et al. 2005; Cuzick et al. 2008). In addition, three different mitogen-activated protein kinase signaling cascades have been demonstrated to contribute to the genetic control of DON trichothecene production (Hou et al. 2002; Urban et al. 2003; Ramamoorthy et al. 2007; Ochiai et al. 2007).

In this study, we describe the use of random insertional mutagenesis to generate a library of hygromycin-resistant (Hyg^r) *F. graminearum* transformants. More than 1,000 transformants were screened on wheat ears and eight reduced-viru-

lence mutants were identified. The pathogenic effects on wheat ear development, mycotoxin production in grain, and root growth have been characterized, along with several in vitro growth and development phenotypes. The precise location of the plasmid integration in the genome of one of these mutants was elucidated using plasmid rescue, sequencing, microarray analysis, and infection of *Arabidopsis* floral tissue. Our data demonstrated that a large block of genes at the end of chromosome 1 are dispensable for many life processes but that this region contains genes conferring full virulence on wheat.

RESULTS

Generation of a library of *F. graminearum* transformants and screening on wheat ears.

A library of 5,000 transformants was generated by random plasmid insertion using two different plasmids to create the transformant population. The plasmid pHA1.3 was originally created as an autonomously replicating plasmid for *F. oxysporum* research and subsequently used for high-efficiency transformation of *Colletotrichum lindemuthianum* (Redman
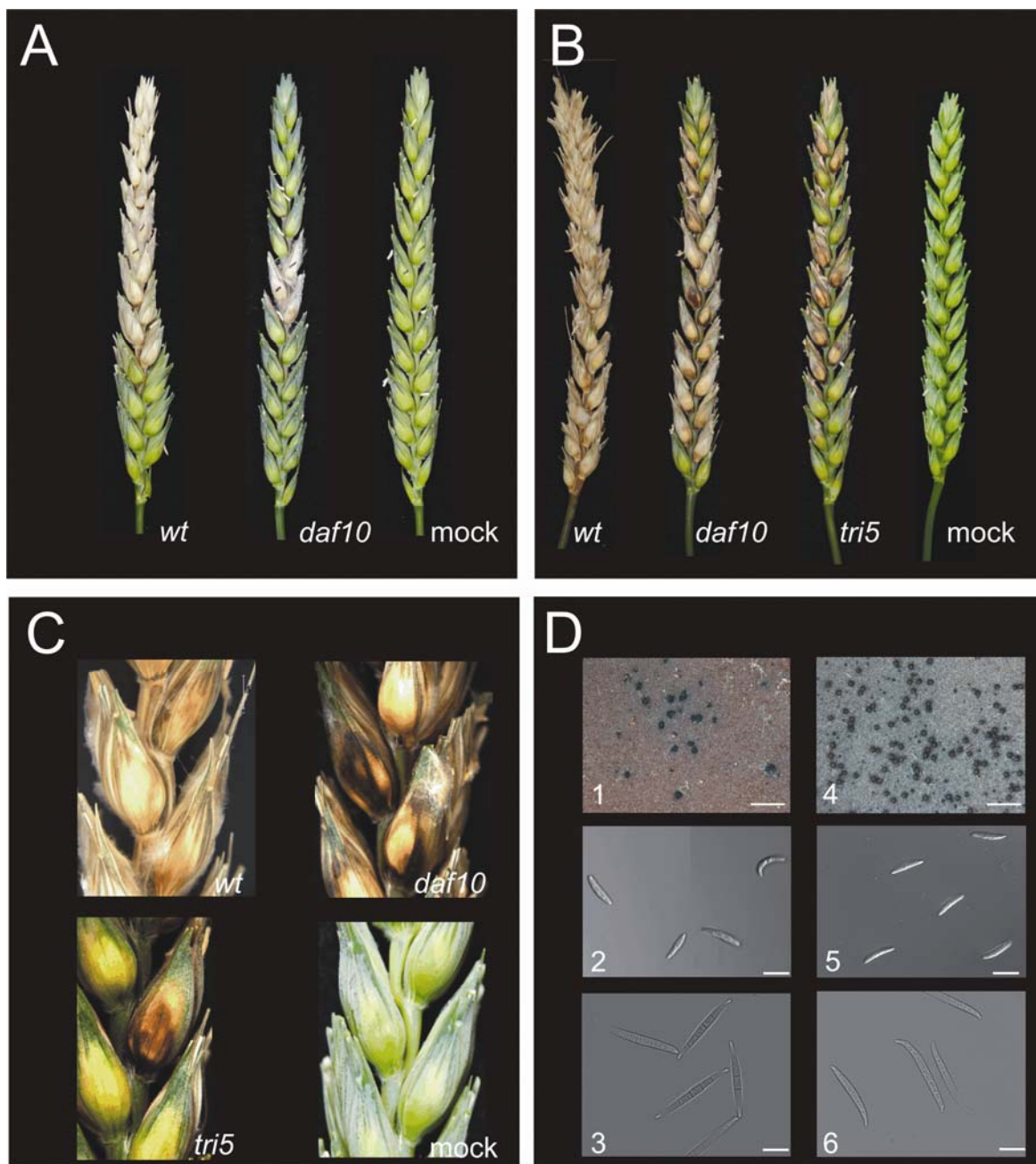

Fig. 1. Comparison of in planta and in vitro phenotypes of the wild-type strain, the *daf10* mutant, and the deoxynivalenol mycotoxin nonproducing *tri5* mutant of *Fusarium graminearum*. **A,** Wheat ears of the susceptible cv. Bobwhite 10 days after point inoculation of two spikelets with either a water droplet containing 200 macroconidiospores or water only. The black pen marks indicate the inoculated spikelets. **B,** Wheat ears 10 days after spray inoculation with a conidial suspension (5×10^4 ml^{-1}). Both the *daf10* and the nontrichothecene-producing *tri5* mutant (also generated in the PH-1 background) produce characteristic eye-shaped lesions on the outer glumes. However, *daf10* causes more severe bleaching of the wheat ear than *tri5*. The ears inoculated with wild-type strain PH-1 have completely bleached. **C,** Close-up of the spray-inoculated spikelets reveals that, although the *daf10* infections result in less symptom development than the wild-type strain PH-1, the *daf10* infections cause tissue browning in the rachis and more severe necrosis on the outer glumes, and develop considerably more aerial mycelium compared with the *tri5* mutant. **D,** In vitro comparison of *daf10* (left column) and wild-type strain PH-1 (right column); 1 and 4, perithecial development on carrot agar; 2 and 5, ascospores; and 3 and 6, macroconidiospores. Bars = 2 mm in 1 and 4 and 20 μm in 2, 3, 5, and 6.

and Rodriguez 1994). This plasmid contains approximately 140 bp of *F. oxysporum* telomeric DNA. The second plasmid, pUCH2-8, contained the hygromycin phosphotransferase (*HPH*) gene fused to promoter 1 from *Cochliobolus heterostrophus* and no telomeric DNA (Turgeon et al. 1987).

A population of Hyg[r] transformants was selected at random from this library for plant infection assays. In total, 1,170 transformants were tested, of which 847 transformants were generated with plasmid pHA1.3 and 323 transformants were generated with plasmid pUCH2.8. Eight transformants were confirmed to be highly reduced in their ability to cause disease symptoms on wheat ears and were named disease-attenuated *F. graminearum* (*daf*) mutants. The *daf* mutants 10, 14, 15, 26, 37, and 38 were generated by pHA1.3, and *daf26* and *daf43* were generated by pUCH2.8. The full infection phenotype of each *daf* mutant was explored in detail by inoculating six flowering wheat ears, of the susceptible cv. Bobwhite, by the point inoculation technique (Table 1). In these infection tests, hyphae of the wild-type parent PH-1 colonized the entire wheat ear within 20 days and caused every spikelet to bleach and the awns to assume a horizontal posture. None of the eight mutants caused visible symptoms on more than half of the entire ear by day 20 postinoculation. After this time, no further visible disease progression occurred (Table 1; Fig. 1). Forty days after inoculation, each ear was harvested and divided into three regions—i) above the point of inoculation, ii) with visible disease symptoms, and iii) below the point of inoculation and without symptoms—and then hand threshed. This revealed the grain number and type recoverable from each region (Tables 2 and 3). This detailed analysis revealed the dramatic effect the

Table 1. Mean number of wheat spikelets with visible disease symptoms 20 days postinoculation

Treatment	Diseased spikelets[z]
Uninoculated	0
Synthetic nutrient-poor agar control	0
PH-1 wild-type	15.33 (±1.21)
daf 10	2.17 (±0.26)
daf 14	5.01 (±1.67)
daf 15	2.33 (±0.82)
daf 26	1.75 (±0.42)
daf 36	2.17 (±0.41)
daf 37	3.75 (±2.60)
daf 38	1.83 (±0.41)
daf 43	4.17 (±3.96)

[z] Values are means ± 1 standard deviation.

Table 2. Impact of *Fusarium graminearum* infection on grain weight and number in the ear

| | Entire ear[w] | | | Per spikelet[w,x] | | | |
| | | | | Region B | | Region C | |
Treatment	Wt (mg)	No.	Spikelets[y]	Wt (mg)	No.	Wt (mg)	No.
None	2,255 c	41.3 b	0	80 c	2.1 c	144 c	2.69 c
SNA only[z]	1,718 bc	37.5 b	0	67.5 bc	1.79 bc	109.38 bc	2.45 c
PH-1	219 a	0.5 a	15.33	0 a	0 a	109.5 bc	1.3 b
daf mutant							
10	1,561 bc	33.5 b	2.17	6.45 a	0.46 ab	92.36 b	2.32 c
14	1,463 b	21.5 ab	5.00	27 ab	1.3 abc	123 bc	2.13 bc
15	1,596 b	15.7 ab	2.33	5.15 a	0.47 ab	112 bc	1.74 ba
26	1,465 b	22.5 ab	1.75	2.86 a	0.28 a	96.08 bc	1.84 bc
36	936 ab	17.3 ab	2.17	0 a	0.32 ab	71.55 b	2.31 c
37	873 ab	23 ab	3.75	11.57 ab	0.85 ab	69.51 b	2.4 c
38	1,277 ab	30.2 b	1.83	2.19 ab	0.44 ab	86.26 b	2.41 c
43	1,506 b	34.5 b	4.17	24.7 ab	1.39 abc	95.44 bc	2.75 c
S^2 at 5%	1,196	27.53	…	60	1.48	51.46	0.94

[w] Wt = grain weight and No. = grain number; values in each column which differ by the letters indicated are statistically significant from each other at the 5% level.

[x] Ear region B, visible disease symptoms and ear region C, no macroscopically visible disease symptoms.

[y] Number of visible disease spikelets.

[z] SNA = synthetic nutrient-poor agar.

Table 3. Impact of *Fusarium graminearum* infection on grain weight, number, and quality in the entire ear and the three different ear subregions (A, B, and C)[x]

| | Region A | | | | | Region B | | | | | Region C | | | | |
| | | | Quality[y] | | | | | Quality[y] | | | | | Quality[y] | | |
Treatment	Wt (mg)	No.	L	M	S	Wt (mg)	No.	L	M	S	Wt (mg)	No.	L	M	S
None	243 b	5.8 abc	86	14	0	160 a	4.2	100	0	0	1,872 b	31.3	98	1	1
SNA only[z]	161 b	4.5 abc	89	4	7	135 a	3.5	90	0	10	1,422 b	29.5	98	0	2
PH-1	0 a	0.4 a	0	0	100	0 a	0	NS	NS	NS	219 a	2.6	0	0	100
daf mutant															
10	362 b	10.8 bc	88	3	9	14 a	1	0	0	100	1,185 ab	30.6	81	9	10
14	98 a	5.3 abc	53	19	28	135 a	6.5	5	18	77	1,230 ab	22	53	43	4
15	165 ab	3.5 ab	62	38	0	0 a	1.1	0	33	66	1,419 b	22.6	52	36	12
26	187 ab	5.5 abc	82	9	9	5 a	0.5	0	0	100	1,273 ab	25	66	24	10
36	18 a	4.5 abc	59	26	15	0 a	0.7	0	0	100	918 ab	30.5	42	18	40
37	48 a	4.3 abc	62	8	30	43 a	3.2	0	0	100	782 ab	27.9	55	13	32
38	13 ab	4.7 bc	50	36	14	4 a	0.8	0	0	100	1,136 ab	32.6	75	9	16
43	74 b	7.3 bc	75	2	23	103 a	5.8	0	23	77	1,129 ab	30.6	70	9	21

[x] Ear region A (constant size), above the point of plug inoculation; ear region B (variable size), visible disease symptoms; and ear region C (variable size), no macroscopically visible disease symptoms or no infection. Wt = mean grain weight per region per ear and No. = mean grain number per region per ear; values in each column which differ by the letters indicated are statistically significant from each other at the 5% level.

[y] Grain quality: L = large, M = medium, and S = small grain, expressed as a percentage of each category; NS = no seed.

[z] SNA = synthetic nutrient-poor agar.

wild-type PH-1 strain had on grain development, whereas most of the *daf* mutant infections permitted more and larger grains to develop within both the symptom and symptomless regions of the ear.

Ability of *Fusarium* mutants to invade root and stem tissues.

A previously established seed germination assay in the presence or absence of *F. graminearum* inoculum (Urban et al. 2003) was used to examine the ability of each *daf* mutant to attack the root and stem base tissue of young seedlings. In the field, this type of infection often arises from *Fusarium* spp.-infected crop residues or from the sowing of infected seed, to cause a seedling blight disease that lowers the initial crop density (Parry et al. 1995).

PH-1 severely impaired seedling emergence to between 14 and 23% of that recovered from the mock-inoculated water controls (Table 4). In the first experimental replicate, aerial seedling biomass 21 days after inoculation was also significantly reduced following PH-1 infection. The eight *daf* mutants with a reduced ability to invade wheat ears at flowering permitted both good seedling emergence and seedling growth in both experimental replicates (Table 4). In experiment 2, where considerably higher levels of disease occurred, three *daf* mutants caused a greater impact on seedling emergence; however, this effect was still considerably less than PH-1.

When the wheat roots were washed free of vermiculite, clear differences between the root systems were visible. Infections by PH-1 caused extreme stunting of the root system, with only two to three short main roots and no lateral roots or root hairs, and roots were a light brown color (data not shown). In contrast, the roots recovered from the mutant-inoculated plants were all large, with many primary, secondary, and tertiary roots, and appeared very similar to those of the mock-inoculated plants. Microscopic examination of trypan blue-stained roots revealed that hyphae of PH-1 had infected the roots and colonized the various tissue layers both intercellularly and intracellularly. In contrast, microscopic observations of roots inoculated with each *daf* mutant failed to identify the presence of fungal mycelium inside root tissue (data not shown). It is possible that small peripheral root infections formed by a mutant were removed when the vermiculite was washed away from the roots and, thereby, lost from the subsequent analyses.

In vitro growth and sexual and asexual spore production.

The in vitro hyphal growth rates were compared on synthetic nutrient-poor agar (SNA) and Vogel's minimal medium agar (VM) for 5 days. No statistically significant differences were evident in the daily rate of hyphal extension on either growth media. For each *daf* mutant, the onset of asexual conidiation, the overall abundance of conidia formed, and the size of conidia on both SNA and VM plates were comparable with that observed for PH-1 (Fig. 1).

Perithecial formation was assessed by growing each *daf* mutant on carrot agar. Seven of the eight *daf* mutants produced normal-size perithecia containing abundant ascospores in an identical manner to PH-1. For *daf38*, perithecia developed after an additional 5 days in culture compared with other mutants and the PH-1 wild-type control (data not shown).

DON and 15-acetyl DON mycotoxin production.

In planta, 15-acetyl DON and DON production was measured by competitive enzyme-linked immunosorbent assay (ELISA) in the hand-threshed grain recovered from each inoculated ear. PH-1 produced DON in all grain samples examined within the range 200 to 405 µg/g dry weight of seed ($n = 9$). The *daf10* mutant produced no detectable DON levels (<0.5 µg/g dry weight of seed). The *daf15*, *daf26*, and *daf38* mutants produced low levels of DON in grain, ranging between 5 and 30 µg/g dry weight, whereas *daf14*, *daf36*, *daf37*, and *daf43* produced wild-type levels. DON production was also investigated in vitro (Table 5) but these results did not correlate well with DON levels in the grain recovered from the inoculated wheat ear. Only *daf36* and *daf43* produced wild-type levels of DON in vitro as well as in wheat grain. The *daf10* and *daf14* mutants produced low DON levels in vitro. The DON amounts detected in cultures of the *daf15*, *daf26*, *daf36*, *daf38*, and *daf43* mutants were in the range of the wild type (Table 5).

Molecular characterization of the *daf10* mutant.

Mutant *daf10*, for which DON was not detected by ELISA in plant material, was selected for DNA gel-blot analysis. The presence of single bands in two different diagnostic digests verified the existence of a single-plasmid insertion event (Supplementary Fig. 1).

A polymerase chain reaction (PCR) assay was designed to test the hypothesis that this no-DON in planta phenotype was due to the disruption of a *TRI* gene in the *TRI5* gene cluster (Kimura et al. 2007). A set of primers specific for the 27-kb *TRI5* gene cluster was designed to amplify the entire *TRI5* locus as six overlapping, approximately 4-kb fragments (Supplementary Table 1). Electrophoresis of the PCR products revealed no size shifts in the expected sizes of any of the products amplified (Supplementary Fig. 2).

Identification of flanking sequences by plasmid rescue.

Two plasmid rescue experiments were done with DNA extracted from *daf10* and digested with *Eco*RV. Nine *Eco*RV colo-

Table 4. Effect of inoculations with *daf* mutants on wheat seed germination and seedling aerial biomass

Treatment	Seed germination (%)		Aerial biomass (g) per germinated seedling	
	Exp. 1	Exp. 2[y]	Exp. 1	Exp. 2
None	100	95	0.24	0.33
SNA[z]	95	100	0.20	0.23
PH-1	24	14	0.10	0.20
daf 10	90	57**	0.15	0.17
daf 14	62	76	0.18	0.22
daf 15	80	38**	0.21	0.30
daf 26	90	76	0.26	0.28
daf 36	80	67	0.19	0.19
daf 37	67	52	0.22	0.31
daf 38	90	86	0.30	0.25
daf 43	90	33**	0.21	0.35
Standard deviation	21	28.5	0.05	0.08

[y] In experiment 2, the overall effect of the disease was higher; ** indicates significantly lower seed germination in experiment 2.

[z] SNA = synthetic nutrient-poor agar.

Table 5. Deoxynivalenol (DON) levels produced in vitro by the wild-type strain and the *daf* mutants

Strain	DON (µg)[z]	
	Rep 1	Rep 2
PH-1	284	71
daf mutant		
10	2.7	4.1
14	2.9	2.6
15	428	400
26	368	123
36	817	244
37	nd	nd
38	179	166
43	203	351

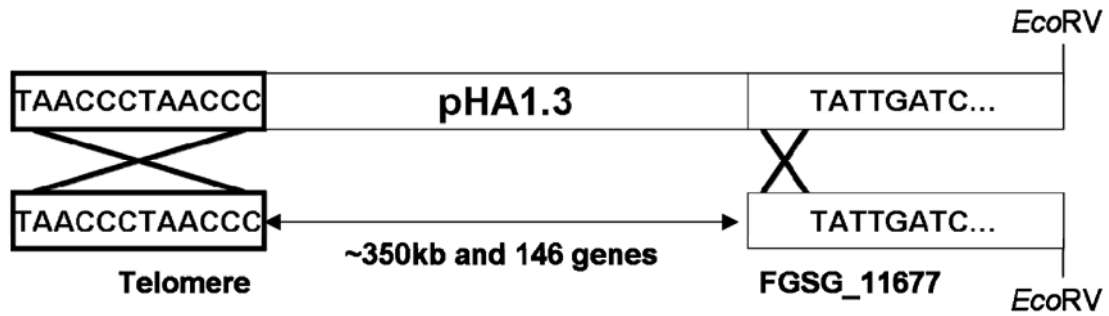[z] Calculated per gram (dry weight) of mycelia; nd = not determined.

Fig. 2. Schematic of the crossover events leading to the *daf10* genotype.
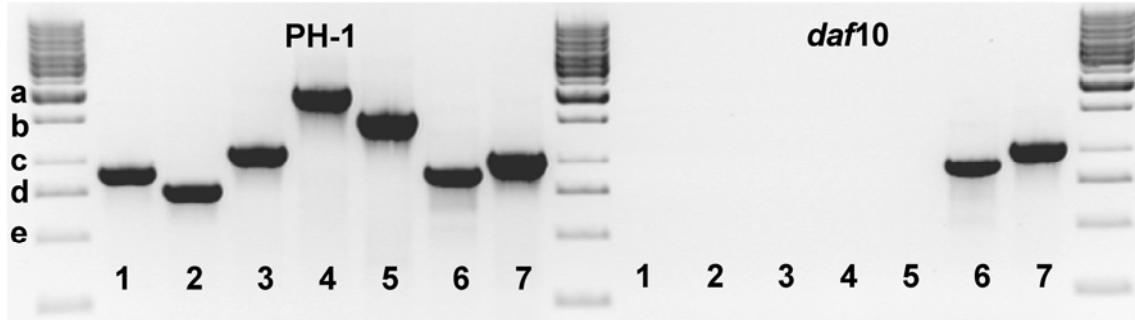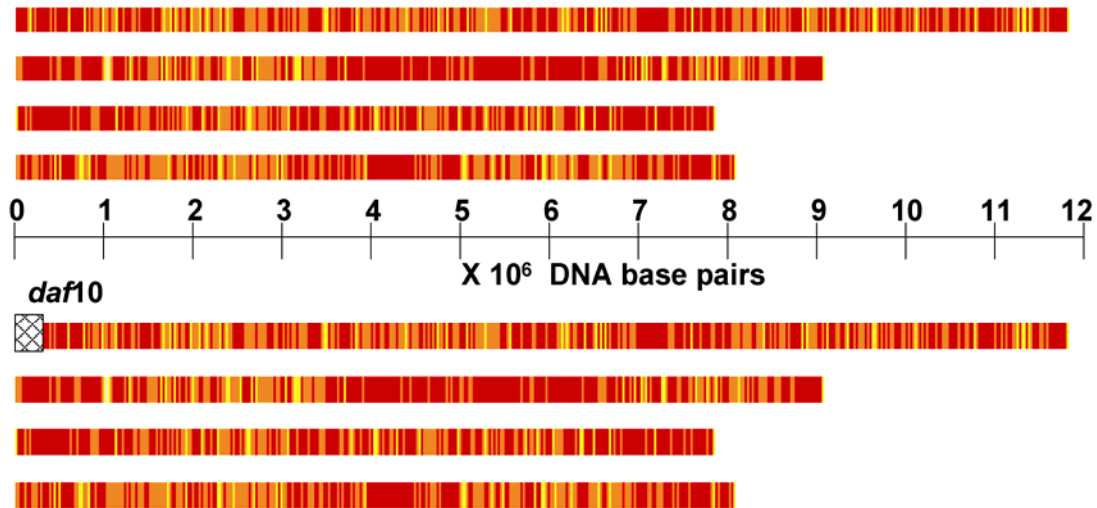

Fig. 3. Polymerase chain reaction analysis of genes predicted to have either been lost or retained on chromosome 1 in *daf10*. Lane 1, FGSG_11579; lane 2, FGSG_00028; lane 3, FGSG_00071 (*TRI1*); lane 4, FGSG_00105; lane 5, FGSG_00092; lane 6, FGSG_11678; lane 7, FGSG_09897. PCR product size ladder: row a, 2,000 bp; row b, 1,500 bp; row c, 1,000 bp; row d, 750 bp; e, row 500 bp.
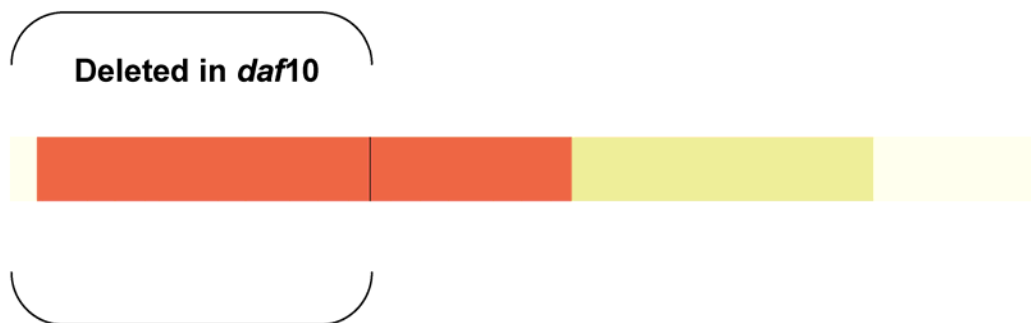
Fig. 4. Gene density and recombination rates of the wild-type (WT) PH-1 and PH-1 *daf10* genomes. **A,** Four chromosomes of PH-1 and *daf10*. Gene density: yellow = <6 genes per 25 kb; orange = 6 to 9 genes per 25 kb; red = >9 genes per 25 kb. **B,** End of chromosome 1 showing the meiotic recombination rates (Gale et al. 2005) and the location of the deletion in *daf10*. Gray background = <1 centimorgans (cM) per 27 kb; beige = 1–2 cM per 27kb; red = 4–8 cM per 27 kb.

nies (pDE1–9) were picked for plasmid extraction and further analysis. When the rescued plasmids were cut with *Pvu*II, there was a clear shift on the gel of approximately 3.5 kb between the total sizes of fragments from the rescued plasmids and the original pHA1.3 plasmid (Supplementary Fig. 3), indicating that additional DNA was associated with the rescued plasmid.

Sequencing of the *daf10* rescued plasmids.

Sequencing primer AMP1 was used to sequence the cloned genomic flanks of the plasmid insertion in the pDE plasmids. Sequencing followed by BLAST analysis revealed that, in *daf10*, one flank of pHA1.3 was within a predicted gene locus located on chromosome 1, namely FGSG_11677. From the second flank of the plasmid, more than 130 bp of telomeric repeat DNA [GGGTTA]$_n$ was recovered. Further sequencing using three different primers (C1.5ANTI1, C1.5ANTI2, and C1.5ANTI3) revealed the exact nature of the plasmid insertion at the FGSG_11677 locus in *daf10*. The integration of pHA1.3 into the PH-1 genome to create the *daf10* transformant appears to have involved two crossover events. The first was a homologous recombination event between the 126 bp of telomeric DNA in pHA1.3 and the *F. graminearum* telomere at the end
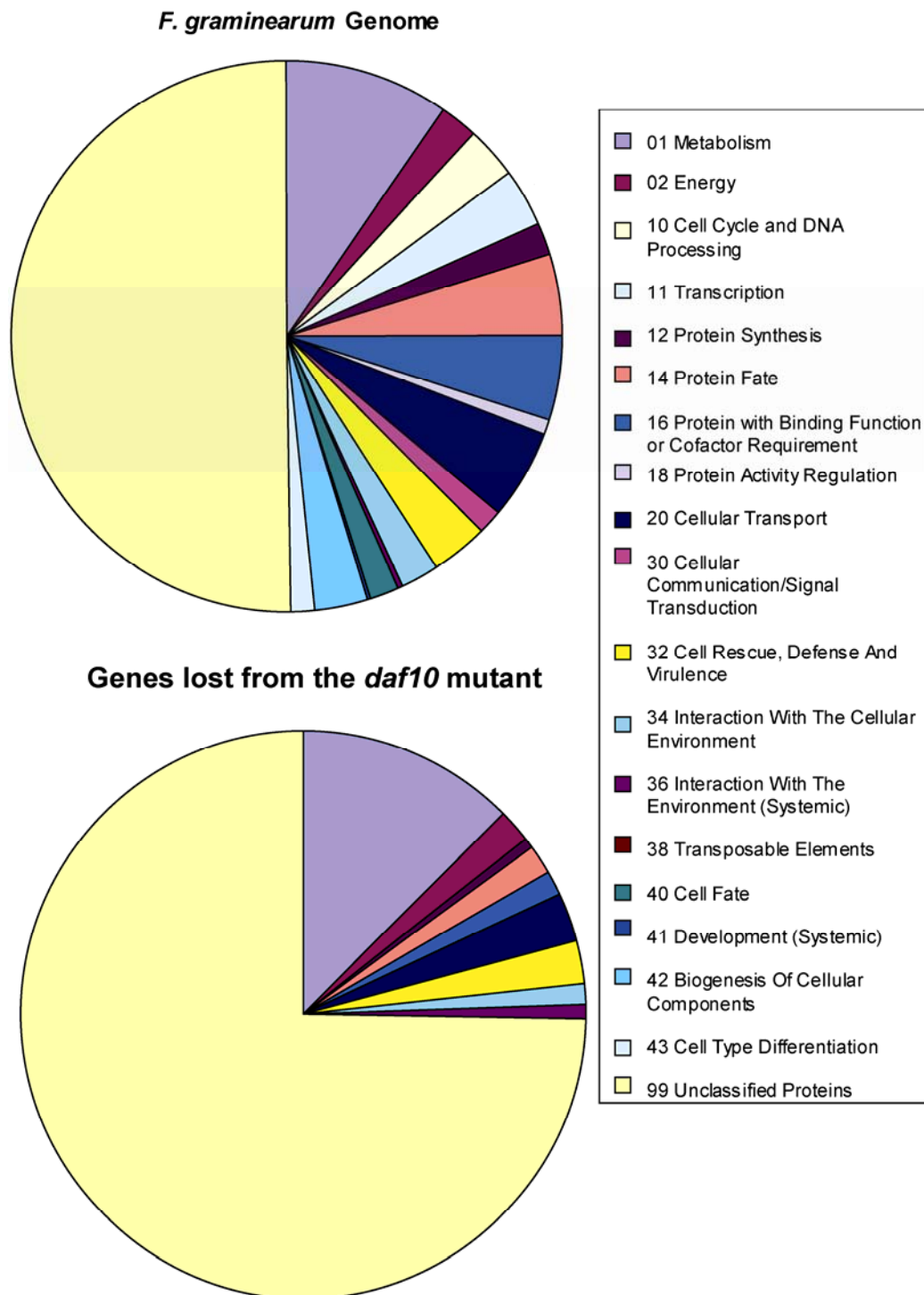

Fig. 5. MIPS functional categorization (FunCat) of the *Fusarium graminearum* genome and of the 146 genes lost from *daf10* mutant. The lower graph shows genes lost from the *daf10* mutant.

of chromosome 1. A second recombination event occurred within the locus FGSG_11677 and did not involve any homology between the end of pHA1.3 and the DNA at the insertion site. This resulted in the deletion of the end of chromosome 1 with the pHA1.3 plasmid replacing approximately 350 kb of DNA and 146 predicted genes (Fig. 2).

PCR evidence of gene loss.

PCR experiments were done to test for the loss of genes predicted to be located in the genome between the plasmid insertion point in FGSG_11677 (coordinates 366,201 to 368,456) and the end of chromosome 1. Primers were designed for five different genes across the deleted region. In addition as a positive control, primers were designed for the gene predicted to now flank the integrated plasmid (FGSG_11678) as well as for a gene located further toward the centromere of chromosome 1 (FGSG_09897). Gel electrophoresis of the PCR products confirmed that genes 1 to 5 had been lost from the genome of *daf10*, whereas the two positive control genes were retained (Fig. 3).

Microarray analysis of *daf10* gene expression.

Further experiments were done to confirm that the 146 predicted genes had been deleted from the genome of *daf10* and to explore the impact of this loss on the expression of predicted genes residing elsewhere in the genome. PH-1 and *daf10* strains were grown under DON-inducing conditions for 7 days as described by McCormick and associates (2004). RNA was extracted from fungal mycelia and hybridized to the *F. graminearum* GeneChip. With one exception, none of the genes predicted to be deleted showed expression in *daf10* (Supplementary Tables 2 and 3). Locus FG00042.1 (Broad FG1 assembly), which was predicted to code for a nonribosomal peptide synthetase, gave a positive hybridization signal on the GeneChip. However, the expression results for the alternative gene model predicted by the Munich Information Center for Protein Sequences (MIPS) (fgd2-360) revealed that the gene at this locus was not expressed in *daf10*. Indeed, the most recent Broad genome assembly (FG3) has resulted in the division of locus FGSG_00042.1 into two different predicted CDS loci; namely, FGSG_11659 and FGSG_11660. Collectively, these results indicate that nonspecific binding had occurred to one or more of the probe sets originally assigned to the locus FG00042.1 in the FG1 assembly. The limits of the deletion are supported by the expression analysis. FGSG_11642 (the third annotated gene in supercontig 1, preceding FGSG_00001; coordinates 9,189 to 9,662) through to FGSG_00100 (coordinates 319,803 to 319,054) are within the low expression (presumed absent) block (data not shown). The first gene with significant expression is FGSG_00476, coordinates 1,472,514 to 1,473,187.

Of the 146 genes predicted to be in the deleted region, 23 genes showed minimal expression in *daf10* compared with PH-1 under DON-inducing conditions. An additional predicted coding region, with so far only expressed sequence tag (EST) support, was also downregulated. Fifteen of the deleted genes have putative annotated function and include a transcription factor (FGSG_00052). In addition, one missing gene, FGSG_00071, is known to code for the cytochrome P450 monooxygenase TRI1. In *F. graminearum*, TRI1 has been shown to be required for the conversion of calonectrin to 8-hydroxylcalonectrin, which is an essential step in DON mycotoxin synthesis. *F. graminearum* strains harboring a disrupted *TRI1* gene accumulate only the 15-decalonectrin and calonectrin precursors under DON-inducing conditions in vitro (McCormick et al. 2004).

These expression experiments revealed that many other genes outside the deleted region also exhibited altered gene expression under DON-inducing conditions. A total of 93 genes had increased expression in *daf10* compared with the wild-type strain. Of these, 31 genes (33%) were annotated. They include two genes involved in trichothecene biosynthesis; namely, FGSG_11025, coding for the transcription factor TRI15, and FGSG_07896, coding for the trichothecene 3-*O*-acetyltransferase TRI101. The transcription factor TRI15 is a known negative regulator of DON mycotoxin production in *F. sporotrichioides* (Alexander et al. 2004) whereas the TRI101 gene product catalyses the transfer of an acetyl group from acetyl coenzyme A to the C3 hydroxyl moiety of several trichothecene mycotoxins. In vitro, this acetyl transfer modification has been shown to reduce the toxicity of these mycotoxins by approximately 100-fold (Kimura et al. 2007). Also upregulated in the *daf10* mutant were three genes related to efflux pumps or transporters. In comparison, only 56 predicted genes and two sequences with only EST support outside the deleted genomic region were downregulated in *daf10* compared with the wild-type PH-1. Of these, 24 (43%) had a predicted function. Further analysis revealed that both up- and downregulated genes in the *daf10* mutant were located on each of the four *F. graminearum* chromosomes and no obvious skewed distribution patterns were evident.

Characterization of the genes lost from *daf10*.

The OmniMapFree software (J. Antoniw, *unpublished*) was used to explore in detail the genetic features and genes which are predicted to reside within the deleted region of chromosome 1 in *daf10*. The gene density in the deleted region was relatively uniform and was similar to the rest of chromosome 1 (Fig. 4A). However in the wild-type strain, this chromosome segment had a region with a very high frequency of meiotic recombination, and a second region with a more modest recombination frequency (Fig. 4B). The crossover event in FGSG_11677 that resulted in the *daf10* deletion occurred in a region with a higher than average rate of meiotic recombination. Next, we explored whether this region contained any homologues of genes predicted to be essential for life in fungi (Nierman et al. 2005). None were found to be present. Then, we explored whether the region contained any homologues of previously characterized pathogenicity and virulence genes in other pathogenic species. This was done by BLASTP analysis using the entire contents of version 3.1 of the Pathogen–Host Interactions database (PHI-base) (Winnenburg et al. 2008). Four PHI-base genes with homologues in the *daf10* deleted region of chromosome 1 with BLASTP *e* values of less than e-100 (Table 6) were identified. An additional 20 PHI-base homologues with a verified role in pathogenicity or virulence with *e* values between e-6 and e-99 were identified in this region. When the PHI-base proteins were queried against the whole *F. graminearum* genome, the top hit resided in the deleted region for only two of the PHI-base proteins (Table 6, indicated in bold).

The functional categorization of the predicted proteins from the *F. graminearum* genome and of the *daf10*-deleted genes was downloaded from the MIPS Functional Catalogue Database (FunCat) version 2.0 (Ruepp et al. 2004). Approximately 50% of the predicted proteins from the whole PH-1 genome are unclassified. Interestingly, approximately 75% of the genes deleted from *daf10* are unclassified. There were also several categories not represented among the deleted genes, including "cell cycle and DNA processing," "transcription," "cell fate," and "biogenesis of cellular components" (Fig. 5).

Further characterization
of the in planta phenotype of mutant *daf10*.

The absence of DON mycotoxin in the grain harvested from the *daf10* mutant-inoculated wheat ears indicated that a

reevaluation of the ear infection phenotype was appropriate. For this analysis, flowering ears were point and spray inoculated with conidia from either wild-type PH-1, *daf10*, or the *tri5* mutant (in the PH-1 background) which is unable to produce DON mycotoxin either in planta or in vitro (Cuzick et al. 2008). The PH-1 strain caused severe ear bleaching, whereas both *daf10* and *tri5* infections caused the formation of eye-shaped lesions (Fig. 1B). However, overall, the *daf10* mutant was more pathogenic than the *tri5* mutant (Fig. 1B and C). Detailed analysis of the infected spikelets indicated that the glume tissue surrounding the *daf10* eye-shaped lesions exhibited some bleaching as well as considerable aerial mycelium development. Also, the rachis tissue adjacent to the *daf10*-infected spikelets turned brown whereas, in the *tri5* mutant–infected ears, the rachis remained green (Fig. 1C).

The phenotype associated with the *daf10* mutant was also compared with that of the previously generated single-gene-deletion *tri1* mutant (McCormick et al. 2004) on *Arabidopsis*

floral tissue. On *Arabidopsis*, the infections of the *daf10* and *tri1* mutants were indistinguishable from each other and from the wild type (Fig. 6).

The in vitro characteristics of mutant *daf10*.

The growth and development of *daf10* was investigated and compared with the wild-type PH-1 strain because of the large gene loss identified. First, fungal growth rates measured as colony diameters were compared on minimal medium, xylan medium, and potato dextrose broth (PDB) agar plates. Linear regression analysis showed that the wild-type strain PH-1 grew slightly faster (1 mm day^{-1}) than the *daf10* mutant on minimal medium (SNA) (Table 7). However, the difference was not significant at the 1% least significant difference (LSD) level. No significant differences were found for fungal growth rates on xylan or PDB medium. Next, we tested the ability to form perithecia, macroconidia, and ascospores. Perithecial formation in the *daf10* mutant and PH-1

Table 6. Pathogen–Host Interactions database (PHI-base) homologues lost from *daf10*[v]

Locus[w]	No. of aa[x]	MIPS annotation	*e* Value	PHI-base[y]	Gene name	Species	PHI-base annotation	Mutant[z]
00006	297	Related to gegh 16 protein	2.74E-60	PHI:257	*GAS2*	*Magnaporthe grisea*	Appressorial penetration	RV
00007	460	Related to *O*-methylsterig-matocystin oxidoreductase	1.24E-06	PHI:438	*BcBOT1 (CND5)*	*Botrytis cinerea*	Cytochrome P450 monooxygenase	RV
00012	519	Related to benzoate 4-monooxygenase cytochrome P450	6.10E-30	PHI:438	*BcBOT1 (CND5)*	*B. cinerea*	Cytochrome P450 monooxygenase	RV
00026	406	Related to monocarboxylate transporter 2	1.21E-53	PHI:812	*MGG_10702*	*M. grisea*	Hypothetical protein	RV
00028	**276**	**Probable metalloprotease MEP1**	**1.40E-66**	**PHI:479**	***MEP1***	***Coccidioides posadasii***	**Metalloproteinase**	**RV**
11654	738	Related to nitrate assimilation regulatory protein	2.51E-06	PHI:169	*CLTA1*	*Colletotrichum lindemuthianum*	Transcription factor	Loss
00036	1,599	Probable fatty acid synthase, α subunit	0	PHI:96	*FAS2*	*Candida albicans*	Fatty acid synthetase	Loss
11655	409	Related to cytochrome P450	2.75E-22	PHI:438	*BcBOT1 (CND5)*	*B. cinerea*	Cytochrome P450 monooxygenase	RV
11656	2,061	Related to FAS1-fatty-acyl-coA synthase, β chain	0	PHI:97	*TOXC*	*Cochliobolus carbonum*	Fatty acid synthetase	RV
11657	741	Conserved hypothetical protein	1.69E-10	PHI:52	*NUT1*	*M. grisea*	Global regulation of nitrogen utilization	RV
11659	4,469	Nonribosomal peptide synthetase	0	PHI:12	*HTS1*	*Cochliobolus carbonum*	Cyclic peptide synthase	Loss
11660	906	NPS8 related to nonribosomal peptide synthetase	1.55E-109	PHI:160	*AMT*	*Alternaria alternata*	AM toxin synthase	Loss
00046	1,446	Related to multidrug resistance protein	3.20E-65	PHI:267	*MLT1*	*Candida albicans*	ABC transporter	RV
00049	383	Related to branched-chain amino acid aminotransferase	2.18E-81	PHI:157	*TOXF*	*Cochliobolus carbonum*	Branched-chain-amino-acid aminotransferase	Loss
00053	382	Probable AAD14 - strong similarity to aryl-alcohol reductase	5.39E-28	PHI:419	*CSH1*	*Candida albicans*	Cell surface protein	RV
00054	310	Conserved hypothetical protein	1.41E-08	PHI:784	*MGG_00056*	*M. grisea*	Unknown	RV
11662	517	Related to L-fucose permease	7.31E-17	PHI:441	*BTP1*	*B. cinerea*	G-protein coupled receptor	RV
00078	328	Related to aldo/keto reductase	5.05E-26	PHI:419	*CSH1*	*Candida albicans*	Cell surface protein	RV
00081	691	Conserved hypothetical protein	3.87E-07	PHI:169	*CLTA1*	*Colletotrichum lindemuthianum*	Transcription factor	Loss
11670	**126**	**Conserved hypothetical protein**	**1.99E-15**	**PHI:489**	***TRX1***	***Cryptococcus neoformans***	**Thioredoxin**	**RV**
11671	842	Related to β-glucosidase	3.49E-38	PHI:24	*Avenacinase*	*Gaeumannomyces graminis*	Avenacinase	Loss
00095	448	Related to tetracycline efflux protein (otrb)	2.14E-28	PHI:60	*TOXA*	*Cochliobolus carbonum*	Toxin pump	Lethal
00101	335	Related to integral membrane protein	4.76E-19	PHI:404	*PTH11*	*M. grisea*	Membrane protein	RV
11677	752	Conserved hypothetical protein	1.91E-78	PHI:672	*CAS1*	*Cryptococcus neoformans*	Capsule polysaccharide biosynthesis	IV

[v] If the FG locus was the top hit in a reciprocal BLASTP of the PHI-base entry against the *Fusarium graminearum* genome, the entry is printed in bold.
[w] *F. graminearum* locus ID (FG3 assembly genecalls FGSG_).
[x] Number of amino acids.
[y] Accession number of top hits in PHI-base by BLASTP.
[z] Mutant defect: RV = reduced virulence, Loss = loss of pathogenicity, and IV = Increased virulence (hypervirulence).

was induced on carrot agar plates as described (Urban et al. 2003). Both the *daf10* mutant and the wild-type strain PH-1 produced black perithecia containing viable and normal-sized ascospores within 2 weeks (Fig. 1D). Macroconidiospore formation and morphology of the *daf10* mutant strain was similar to the wild type (Fig. 1D, panel 2 and 5). The germination of macroconidiospores was assessed by pipetting spores of *daf10* and the wild-type in SNA agarose medium on microscope slides and then incubating for 12 h at 22°C. No significant difference in germination rates between PH-1 and the *daf10* mutant was detected in four replicate experiments (means of 0.97 ± 0.05 and 0.96 ± 0.01, respectively). In summary, the *daf10* mutant showed no significant defects in growth rates, perithecial formation, spore formation, and germination.

DISCUSSION

This study used a forward genetics approach and identified eight *F. graminearum* transformants with significantly reduced pathogenicity on wheat ears and roots. The transformant *daf10*, which appeared initially to harbor a single plasmid insertion event, was selected for detailed characterization. These analyses revealed the presence of a highly complex genomic alteration which led to the loss of 146 predicted genes from the end of chromosome 1 of *daf10*. In vitro, the mutant

Table 7. Comparison of growth rates of the *daf10* mutant and wild-type strain in minimal medium (synthetic nutrient-poor agar.[SNA]) and two complete media (xylan and potato dextrose broth [PDB])

	Growth on culture medium (mm day^{-1})^z		
Strain	SNA	Xylan	PDB
daf-10 mutant	17.35	18.20	17.85
PH-1	18.43	17.50	17.63

^{z} Mean growth rate measured as colony diameters ($n = 4$). Linear regression was applied to estimate the diameter growth rate for each colony. Analysis of variance revealed a marginally significant interaction between media and strains ($P = 0.022$, F test). The standard error of difference of the mean for the strain – media interaction is 0.420 on 18 d.f. No significant differences for the means were found at the 1% least significant difference level, which was 1.209.

daf10 grew normally and produced both sexual and asexual spores. On wheat ears, no trichothecene mycotoxin production was detected but the *daf10* infection phenotype was slightly more severe than that of the *tri5* or the *tri1* mutant whereas, on *Arabidopsis* floral tissue, both *tri1* and *daf10* mutants exhibited wild-type pathogenicity. A microarray experiment done to explore gene expression under DON-inducing conditions revealed that the *daf10* mutant also exhibited a considerably altered transcriptomic profile, involving both the increase and decrease in abundance of transcripts arising from genes located in other genomic regions.

The plasmid used to generate *daf10*, pHA1.3, was created for high-efficiency transformation of *Colletotrichum lindemuthianum* (Redman and Rodriguez 1994). This plasmid, originally recovered from an *F. oxysporum* transformant using the plasmid pFOLT4R4, contains *Fusarium* telomeric DNA as a result of an in vivo modification (Powell and Kistler 1990). A derivative of pFOLT4R4 which also retained this telomeric DNA (pLD) had previously been used to transform *Nectria haematococca* (anamorph: *F. solani*) and many of the resulting transformants were noted in pulsed-field gel electrophoresis analysis to have been subjected to large chromosomal deletions, up to 2 MB in some cases (Kistler and Benny 1992). The plasmid was originally chosen for mutagenesis because of the higher recovery rate of transformants, which appeared to be stable in initial tests of successive transfers.

By using the OmniMapFree software which links genome sequence information directly to the genetic map, we were able to explore the genome location surrounding the plasmid insertion that had occurred in the predicted gene FGSG_11677. This gene is in a genomic region that exhibits a higher than average level of meiotic recombination in a cross between strains PH-1 and a second American strain, MN00-620 (Gale et al. 2005), and is in a region of high single nucleotide polymorphism (SNP) occurrence (Cuomo et al. 2007). Double-strand breaks are created during meiotic recombination (Cao et al. 1990) and, in *Saccharomyces cerevisiae*, these breaks have been demonstrated to occur at specific chromosomal hotspots (Gerton et al. 2000).

The published, sequenced genome for the *F. graminearum* PH-1 lacks all eight telomeric regions. Therefore, although the predicted gene loss in the *daf10* mutant is currently 146 genes,
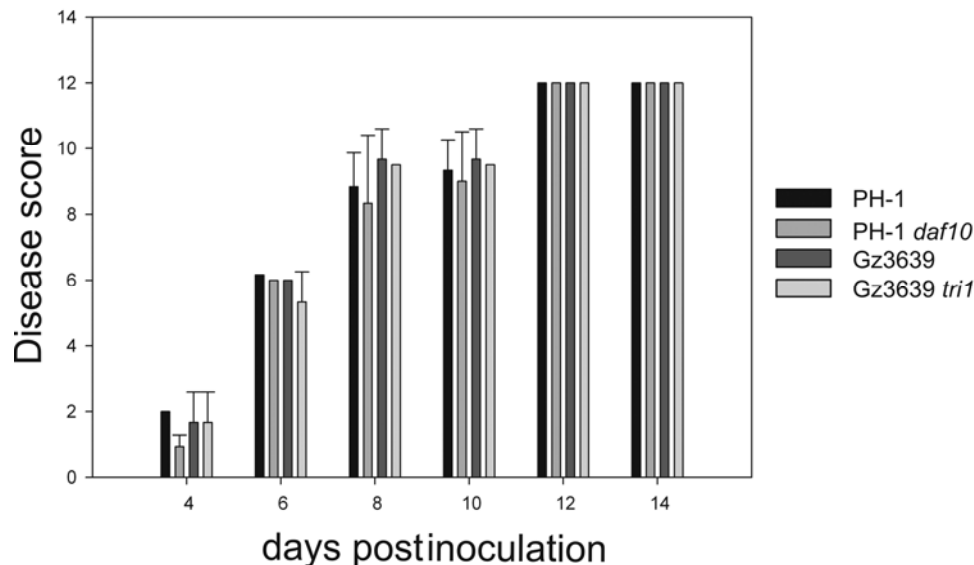

Fig. 6. Development of *Fusarium graminearum* infection on *Arabidopsis* ecotype Landsberg erecta floral tissue by the *daf10* and *tri1* mutants and the respective wild-type strains. Disease scores for the flowers and new siliques were assessed separately and then combined. Error bars indicate standard deviation ($n = 12$).

this number may rise once the full genomic sequence becomes available. The wild-type growth characteristics of *daf10* and its ability to grow vegetatively and to produce both sexual and asexual spores indicates either that none of the deleted genes have significant roles in *Fusarium* cell development or, alternatively, that their absence can be compensated for by genes residing in other parts of the genome. Our detailed bioinformatics analyses of the deleted region tends to indicate that the former view is the more likely explanation for the viability of the *daf10* mutant because no genes "essential for life" were predicted to reside within this region. Also, no genes were predicted within four key gene ontology categories; namely, "cell cycle and DNA processing," "transcription," "cell fate," and "biogenesis of cellular components". Double-stranded breaks are normally highly deleterious, and organisms contain pathways to specifically suppress these events (Lee and Myung 2009). The tolerance of *F. graminearum* to this deletion provides the first functional evidence that nonessential genes are clustered in the telomeric regions. These regions have higher apparent variability, as suggested by SNP analysis, and many are species specific (Cuomo et al. 2007).

The precise pathogenicity defects in the *daf10* mutant are difficult to predict beyond the loss of *Tri1*. At least 20 genes were found to have some level of homology with known pathogenicity and virulence genes in other plant- or animal-infecting fungi. Alternatively, the defect may be conferred by one or more of the numerous unannotated genes. In *F. graminearum*, 23 genes have been shown thus far, through gene deletion or gene disruption experiments, to contribute to pathogenicity or virulence on wheat ears (Baldwin et al. 2006; Winnenburg et al. 2008). Interestingly, all these genes reside within regions of the genome which have either low or no recombination (Cuomo et al. 2007; Beacham et al. 2009; J. Antoniw, A. M. Beacham, M. Urban, and K. E. Hammond-Kosack, *unpublished*), whereas the deleted genomic region in the *daf10* mutant exhibits either a high or a moderate level of recombination. Although others have suggested that genes which reside within the subtelomeric regions of *F. graminearum* play a role in pathogenicity due to the observation that there is a preferential enrichment of in planta expressed genes in these genomic regions (Cuomo et al. 2007), this is the first direct evidence for such a role. The wheat seedling root assay results also indicate that a gene residing in this subtelomeric region also contributes to root colonization and pathogenesis, whereas the *Arabidopsis* floral inoculation results suggest that none of the genes residing within the deleted chromosomal region contribute to virulence toward this dicotyledonous host species, unless the simultaneous and balanced loss of both positive and negative regulators of pathogenicity has occurred in the *daf10* mutant.

The macroscopic *daf10* disease phenotype on wheat ears was an unexpected result of this mutant. Although the number of colonized spikelets following point inoculation was minimal—typically, only those inoculated and their immediate neighbors exhibited disease symptoms—the glumes of each spikelet were not fully bleached. Instead, an eye-shaped lesion formed which was surrounded by limited glume bleaching and browning of the neighboring rachis tissue whereas, when the *tri5 F. graminearum* mutant in the PH-1 genetic background infected the identical susceptible wheat genotype, only a dark border developed at the edge of the infection, and an eye-shaped lesion without bleaching of the surrounding glumes or browning of the rachis occurred (Fig. 1B and C). These contrasting in planta results indicate that, in the absence of DON accumulation, the *daf10* mutant disease phenotype is greater than that of the *tri5* mutant (Cuzick et al. 2008). This would suggest that the product from another gene residing within the

deleted chromosomal region is directly or indirectly responsible for limiting growth (or contributing to growth) in wheat ears. Alternatively, DON production may just be very low in the *daf10*-infected spikelets and, although able to induce eye-shaped lesion formation on the glumes accompanied by some glume bleaching, this infection does not lead to DON accumulation at significant levels in the developing grain.

The *TRI1* gene had been deleted from *daf10*. This gene, which codes for a cytochrome P450 monooxygenase, has previously been demonstrated to be essential for DON biosynthesis during in vitro growth of *F. graminearum*; however, the effects of this gene deletion on pathogenicity had not been reported (McCormick et al. 2004). Therefore, we compared the pathogenicity of this *tri1* mutant in the Gz3639 genetic background with the *daf10* mutant on both wheat ears and *Arabidopsis* floral tissue. The later pathosystem was included because a previous study had reported that DON production does not contribute to *F. graminearum* pathogenicity of *Arabidopsis* (Cuzick et al. 2008). The *tri1* mutant, like *daf10*, exhibited highly reduced pathogenicity on wheat ears and caused the formation of eye-shaped lesions. However, there were some subtle differences in the phenotypes of the *daf10* and *tri1* mutants on wheat ears, with the *daf10* mutant showing slightly more severe symptoms (Supplementary Fig. 4). It must be noted that the different parental backgrounds of these two mutants cannot be absolutely eliminated as the cause of these phenotypic differences. Both *daf10* and *tri1* mutants caused wild-type infections on *Arabidopsis* buds, flowers, siliques, and upper stem tissue. Mutations in the *TRI1* gene are known to cause the accumulation of calonectrin and 3-decalonectrin in *F. graminearum* (McCormick et al. 2004). *Arabidopsis* has been shown to be highly sensitive to these two compounds, with 3-calonectrin (50% effective dose 7.6 ± 1.4 μM) only slightly less toxic than DON (3.8 ± 3.0 μM) (Desjardins et al. 2007). The probable accumulation of calonectrin derivatives in the *daf10* mutant would explain the wild-type pathogenicity effect on *Arabidopsis* and the reduced pathogenicity on wheat.

A recent report by Gardiner and associates (2009) used the Fusarium GeneChip to do a global analysis of fungal gene expression after 4 days under DON-noninducing and DON-inducing conditions generated by amine compounds in culture (glutamine versus agmatine, respectively). The survey identified many genes which were differentially regulated under these conditions. One of the genes highly induced under their DON-inducing conditions, namely FGSG_00007, which is on the lost arm of the chromosome in *daf10*, was selected for gene disruption. This mutation resulted in increased DON production (14-fold) and increased aggressiveness toward wheat ears manifested as a greater rate of spread from spikelet to spikelet. The FGSG_00007 locus is predicted to encode a putative cytochrome P450 monooxygenase. In this study, the Fusarium GeneChip analysis were done after 7 days of growth under DON-inducing conditions and FGSG 00007 was not found to be differentially expressed. Gardiner and associates (2009) hypothesized that the product of FGSG_00007 may be involved in the negative regulation of DON biosynthesis. Thus, the *daf10* mutant originally selected on the phenotype of reduced aggressiveness toward wheat ears and low or no DON mycotoxin accumulation combines the loss of this negative regulator with the loss of an essential step in DON biosynthesis. This probably explains why subtle differences were consistently observed between the *tri1* mutant and *daf10* mutant phenotypes, which could possibly be the result of an increased accumulation of calonectrin derivatives. An increased amount of these compounds may explain the increased virulence on wheat glumes of *daf10*. In addition, the loss of FGSG_00007

resulted in increased production of other secondary metabolites (Gardiner et al. 2009), which may also render *daf10* more virulent than the *tri1* mutant. The FGSG_00007 mutant exhibits moderately increased virulence when point inoculated into cv. Bobwhite wheat ears compared with the parental wild-type strain CS3005 (G. Canning, Rothamsted Research, *unpublished*). Once the FGSG_00007 gene loss is available in the same parental background as the *daf10* mutant (namely, strain PH-1), these biological and possible biochemical differences can be fully examined.

The microarray analysis of the *daf10* mutant under DON-inducing conditions in vitro revealed that many additional genes located across the four *F. graminearum* chromosomes were specifically either up- or downregulated compared with the wild-type strain. Overall, considerably more gene transcripts were detected in increased abundance in the *daf10* mutant (93 increased versus 58 decreased), suggesting that some genome-wide positive transcriptional compensation was required to counter the presence of this sizeable genome deletion, which contains at least 146 genes. However, the global changes observed for the *daf10* mutant were less than when single-gene-deletion strains lacking either the transcription factors TRI6 or TRI10 were explored under the same DON-inducing conditions (Seong et al. 2009).

The analysis of the *daf10* mutant clearly indicates how invaluable the emerging new tools and resources for *F. graminearum* are to the detailed characterization of mutants which resulted from a complex integration event. This analysis was only possible because of the availability of full genomic sequence information linked to a genetic map as well as a near-full genome microarray. The technique of random plasmid insertion combined with a forward genetic screen remains a very valuable approach to the discovery of novel pathogenicity and virulence genes. However, a proportion of the recovered mutants typically have multiple copy insertion events which makes the downstream analysis to recover the gene conferring the phenotype of interest difficult and time consuming. The analysis of multi-insertion mutants either singly or by pooling, via a combined microarray and high-throughput sequencing study, would be a rapid and informative way to distinguish between clean and "multicopy" insertion events, which could easily then be investigated by targeted single-gene-deletion experiments, from those which have led to either minor or more major genome rearrangements that would be more difficult to characterize further.

MATERIALS AND METHODS

Strains and growth conditions.

The strain Gz3639 was obtained from the United States Department of Agriculture stock culture collection (NRRL29169) whereas strain Gz3639 *tri1* was obtained from the Fungal Genetics Stock Center Strains (FGSC 9501). *F. graminearum* PH-1 (FGSC 9075) was isolated from infected wheat in Michigan (Trail and Common 2000). Both Gz363 and PH-1 belong to genetic lineage group 7 (O'Donnell et al. 2000) and a whole-genome sequence is available (Cuomo et al. 2007). Both the wild-type and transformed strains were maintained as soil stocks at –20°C. All isolates were routinely cultured on SNA plates containing 0.1% KH$_2$PO$_4$, 0.1% KNO$_3$, 0.1% MgSO$_4$ × 7 H$_2$O, 0.05% KCl, 0.02% glucose, 0.02% saccharose, and 2% Bacto Agar (Becton, Dickenson and Company, Sparks, MD, U.S.A.) at 22°C under continuous white and blue fluorescent lights. Macroconidia for plant inoculation experiments were harvested from 10-day-old SNA agar plates. Perithecia production was induced on carrot agar (Trail et al. 2003).

Vectors for transformation of *F. graminearum*.

Plasmid pHA1.3 was constructed with the hygromycin B phosphotransferase gene (*hph*) linked to the *Aspergillus parasiticus trpC* promoter and terminator sequences. In addition, this plasmid has a telomeric region from *F. oxysporum* inserted downstream of the *trpC* terminator (Redman and Rodriguez 1994).

Fungal transformation.

Transformations were done on germinated conidia using a previously published protocol (Proctor et al. 1995) with the following modifications. Approximately 0.3 g of a soil stock was used to inoculate carboxymethylcellulose (CMC) medium and incubated for 72 h at 25°C at 250 rpm. Conidia were harvested by centrifugation and germinated in YEPD broth (0.3% yeast extract, 1% bactopeptone, and 2% D-glucose) for 12 to 14 h at room temperature at 175 rpm. Isolation of protoplasts occurred in driselase at 25 mg/ml, chitinase (Sigma-Aldrich, St. Louis) at 0.05 mg/ml, and either mureinase (USB-Amersham Pharmacia Biotech Inc., Piscataway, NJ, U.S.A.) at 0.5 mg/ml or lysing enzyme (Sigma-Aldrich) at 5 mg/ml in a 1.2 M KCl buffer. Protoplasts were collected by filtration through a 30-μm Nitex nylon membrane (Tetko Inc., Kansas City, MO, U.S.A.) and washed three times in STC buffer (1.2 M sorbitol, 10 mM Tris-HCl, and 50 mM CaCl$_2$, pH 8.0). Transformation took place in the presence of 30% polyethylene glycol solution (10 mM Tris-HCl, 50 mM CaCl$_2$, pH 8.0), STC buffer, and linearized plasmid. Protoplasts recovered on regeneration medium (RM) (0.1% yeast extract, 0.1% casein enzyme hydrosylate, 0.8 M sucrose, and 1% agarose) for 15 h and then were overlaid with 10 ml of RM amended with hygromycin B (HygB) at 150 μg/ml (Calbiochem-Novabiochem Corp., San Diego, CA, U.S.A.). Putative transformants were selected within 4 to 7 days and retested for hygromycin resistance on V8 juice medium amended with HygB at 450 μg/ml. Hyg^r colonies were transferred to a 2% water agar medium and hyphal tipped to obtain genetically pure isolates.

Infection assays on wheat plants.

Preliminary screening of the population of *Fusarium* transformants was carried out on greenhouse-grown wheat cv. Norm. Seeds (four per 6-in. pot) were sown in high-porosity professional planting mix (Michigan Peat Company, Houston). Plants were fertilized weekly, starting 2 weeks after germination, until they reached the boot stage. Plants at early anthesis were selected for inoculation. Each *F. graminearum* transformant was grown in liquid carboxymethylcellulose medium to generate conidia as previously described (Guenther and Trail 2005). Plants were inoculated by placing 10 μl of the spore suspension (10^5 spores/ml) within the floral chamber of a floret midway along the ear. Two plants were inoculated with each transformant and PH-1 was inoculated similarly on other ears as controls. The plants were placed in a misting chamber (misting frequency 10 s every 6 min) for 72 h and then returned to standard greenhouse conditions. Wheat ears were assessed 8 to 13 days postinoculation for development of symptoms relative to that of PH-1. Symptoms observed were the extent of bleaching on the ears (two or more spikelets from the point of inoculation), deformation of the awn, and extent of seed set. If one of the two ears showed these symptoms, the strain was considered pathogenic.

For the secondary screen, seed of spring wheat cv. Bobwhite was sown in Levingtons C2 coarse potting compost. Seedlings were transplanted singly into 10-cm pots and grown for an additional 2 months in a controlled environment growth room at 18°C during the 16-h day and 16°C during the 8-h night, at 50% relative humidity. Light was supplied by a mixture of metal hyalide and incandescent lamps to produce a fluence

level of 207 microM at 86.2 W/msq at the plant surface. Once the plants entered anthesis, individual attached ears were selected that bore two to five spikelets with extruded anthers. A small agar plug (2 mm in diameter) cut from the hyphal edge of each *Fusarium* insertional mutant growing on SNA media was then inserted into a single floret within the first full-sized spikelet down from the ear apex (Fig. 1). A second hyphal agar plug was inserted into an adjacent spikelet. The glumes of the two inoculated spikelets were marked with a waterproof pen. After inoculation, the entire plant was placed into a high-humidity chamber (>95% relative humidity) for the next 3 to 4 days. Light was excluded from the plants for 16 h postinoculation. The plants were then returned to the standard growth room conditions. Wheat ears were assessed at 4, 8, 12, 16, and 20 days postinoculation for disease. Disease symptoms were quantified by i) counting the total number of spikelets at and below the point of inoculation exhibiting bleaching symptoms, ii) noting the extent of brown streaking on the rachis segments below the point of inoculation, and iii) examining the ear region above the point of inoculation for bleaching. A minimum of six ears was inoculated for each insertional isolate and the same number of control PH-1 inoculated ears were included within each batch of inoculations.

The ability of each transformant with a reduced ability to cause ear blight symptoms to invade young wheat seedlings was explored by germinating Bobwhite wheat seed in a mixture of vermiculite and transformant hyphae. A 50-ml plastic container tube with drainage holes at the base (Steuwe and Sons, Inc, Oregon, OR, U.S.A.) was two-thirds filled with moist sterile vermiculite. Into the top surface was incorporated one-eighth of an entire 7-day-old SNA plate (diameter, 10 cm) of a *Fusarium* isolate that had been chopped into small pieces (5 mm³). Three Bobwhite wheat seeds, from a stock known to give 100% germination, were placed onto the surface of the vermiculite/hyphal agar surface; then, a further 15 ml of moist sterile vermiculite was added to completely cover the seeds. Seven identical containers were set up for each insertional *Fusarium* isolate tested. The finished containers were placed vertically in racks. Control containers were established with SNA agar only. To each container was added 10 ml of water every second day for the 7 days and then daily thereafter. At 14 days after sowing, each container was scored nondestructively for seedling emergence. At 21 days after sowing, each container was disassembled, the vermiculite gently washed from the root system, and the roots scored for browning discoloration and physical appearance. In addition, the aerial parts of the emerged seedlings above the first leaf sheath were excised and the fresh weight determined. The experiment was repeated on two separate occasions.

Root tissue samples were taken at 21 days after inoculation from each insertional *Fusarium* isolate interaction. Conventional histochemical staining of fungal hyphae was performed using lactophenol-trypan blue and destaining with chloral hydrate (Keogh et al. 1980). Microscopic observations were made on a Carl Zeiss Axioskop 2 instrument under phase contrast.

Infection assays on *Arabidopsis* plants.

These assays were done by spray inoculation of conidia onto floral tissue of *Arabidopsis thaliana* accession Ler-0 using previously described methods (Cuzick et al. 2008). Twelve plants were sprayed with each *Fusarium* genotype or with water as a control.

In vitro growth tests and microscopy.

To measure fungal growth rates, mycelium plugs from 1-week-old cultures on SNA minimal agar plates were transferred onto fresh agar plates using an 8-mm cork borer. Fungal growth was recorded as colony diameter in daily intervals over 5 days, which was prior to any colony reaching the edge of its dish. Germination of macrospores was assessed by embedding spores in SNA soft agarose on a microscope slide. SNA medium containing 0.7% low-melting-point agarose was cooled to 30°C and mixed with 5×10^4 spores ml^{-1}. A 300-μl aliquot of the spore mix was then used to coat a microscope slide with a thin layer of the agarose-spore medium. Coated slides were transferred to a high-humidity chamber at 22°C and germination was evaluated after 12 h. A Zeiss Axiophot light microscope was used to examine spore morphology, size, and germination at higher magnifications. Perithecial formation on carrot agar plates was analyzed using a Leica MZFIII dissecting microscope.

Competitive ELISA detection of DON and 15-acetyl DON.

To induce trichothecene production, strains were grown in triplicate on liquid DON-inducing medium as previously described (McCormick et al. 2004). Samples from medium were recovered after 7 days of growth. Quantitative combined DON and 15-acetyl DON measurements were made using the commercial Veratox 5/5 kit (Neogen Corp., Lansing, MI, U.S.A.) and deploying a standard curve for DON ranging from 0.25 to 3.00 ppm. Optical densities at 650 nm values were measured after the addition of the stop solution to the multiwells. To ensure accuracy, each biological sample was quantified twice for combined DON and 15-acetyl DON levels.

DNA gel blot analyses.

Genomic DNA from various *daf* mutants and the PH-1 wild-type strain was extracted and digested with three different restriction enzymes which were predicted to cut either within the *hph* gene (*Eco*RI) or within the inserted plasmid (*Sph*I and *Mlu*I). The digested DNA was separated by size on large electrophoresis gels and blotted onto separate membranes (Hybond N⁺) using an alkali Southern blotting technique (Sambrook et al. 1989).

The DNA gel blot membranes were probed with a PCR-amplified fragment of the *hph* hygromycin resistance gene labeled with radioactive ³²P. The DNA probe specifically hybridized with two fragments in the *Eco*RI-digested DNA gel blot, consistent with a single plasmid insertion. The *Eco*RI restriction enzyme is predicted to cut once within the *hph* gene, thereby generating two fragments.

PCR, plasmid rescue, and sequencing.

HotstarTaq (Qiagen, Hilden, Germany) was used for reactions with *Fusarium* genomic DNA. Reactions were done with volumes of 25 μl in 200-μl polypropylene PCR tubes with an Applied Biosystems (Warrington, U.K.) GeneAmp 9700 thermocycler. A Fermentas 1-kb Generuler was used to identify PCR product sizes in the subsequent agarose gel analyses.

A plasmid rescue technique described by Kuspa and Loomis (1992) was applied to isolating the flanking regions of plasmid pHA1.3 integrated into the genomic DNA of the *daf10* mutant during protoplast.

Sequencing reactions were done with ABI Big Dye terminators V1.1 (Applied Biosystems). Sequencing reaction products were purified using an ethanol/sodium acetate method recommended by Applied Biosystems to remove unincorporated dye terminators. The extension products were sequenced on an ABI Prism 3730xl DNA Analyser (University of Oxford, DNA Sequencing Facility, Oxford).

Microarray analyses.

Expression analysis was performed on DON-induced cultures grown as described above. RNA was extracted from three

replicates of *daf10* and two replicates of wild-type PH-1 using the Trizol (Invitrogen, Carlsbad, CA, U.S.A.) cetyltrimethylammonium bromide–chloroform protocol reported by Hallen and associates (2007), followed by cleanup using RNeasy (Qiagen) following the manufacturer's directions. These RNAs were used to query Affymetrix Fusariuma520094 GeneChips (Güldener et al. 2006) following standard protocols (Affymetrix 2004). The hybridization signals were scanned with a GeneChip GCS 3000 Scanner (Affymetrix) and the cell intensity (CEL) files were obtained from GCOS 2.1 software (Affymetrix). CEL files were normalized in the Bioconductor package of R, version 2.3.0rc (Gentleman et al. 2004, R Development Core Team 2006), using RMA, an expression measure that accounts for background correction, quantile normalization, and variation between arrays (Irizarry et al. 2003a,b). Comparisons between *daf10* and the wild type were conducted using the Limma package of Bioconductor (Smyth 2005; Hallen and Trail 2008). Statistical significance was empirically determined by selecting the cutoff *P* value lower than the smallest *P* value found in any of the Affymetrix control probe sets, as recommended by Smyth (2005). Microarray data and CEL files are available at Plexdb as FG17.

Other statistical analyses.

The one-sample *t* test was used to identify statistically significant differences between two populations. One-way analysis of variance (ANOVA) with blocking was used to identify LSD between more than two populations. The computer program Genstat, version 9.2 (VSN International, Oxford), was used for these statistical calculations. The Microsoft Excel computer program was used for calculating means, standard deviations, and *P* values for the χ^2 test.

A two-stage analysis was used to analyze the growth rates of fungal colonies. First, diameters of the colonies were plotted against time for each replicate dish and were found to increase linearly. Linear regression was applied to estimate the diameter growth rate (millimeters per day) for each colony. For the second stage of the analysis, ANOVA was used to consider the significance of differences between the treatment combinations (media–strains). Following the ANOVA, means were compared using the LSD at the 1% level of significance.

ACKNOWLEDGMENTS

LITERATURE CITED

Affymetrix. 2004. GeneChip expression analysis. Affymetrix, Santa Clara, CA, U.S.A.

Alexander, N. J., McCormick, S. P., Larson, T. M., and Jurgenson, J. E. 2004. Expression of *Tri15* in *Fusarium sporotrichioides*. Curr. Genet. 45:157-162.

Baldwin, T. K., Winnenburg, R., Urban, M., Rawlings, C., Koehler, J., and Hammond-Kosack, K. E. 2006. The pathogen-host interactions database (PHI-base) provides insights into generic and novel themes of pathogenicity. Mol. Plant-Microbe Interact. 19:1451-1462.

Beacham, A. M., Antoniw, J., and Hammond-Kosack, K. E. 2009. A genomic fungal foray. Biologist 56:98-105.

Cao, L., Alani, E., and Kleckner, N. 1990. A pathway for generation and processing of double-strand breaks during meiotic recombination in *Saccharomyces cerevisiae*. Cell 61:1089-1101.

Cuomo, C. A., Güldener, U., Xu, J. R., Trail, F., Turgeon, B. G., Di Pietro, A., Walton, J. D., Ma, L. J., Baker, S. E., Rep, M., Adam, G., Antoniw, J., Baldwin, T., Calvo, S., Chang, Y. L., DeCaprio, D., Gale, L. R., Gnerre, S., Goswami, R. S., Hammond-Kosack, K., Harris, L. J., Hilburn, K., Kennell, J. C., Kroken, S., Magnuson, J. K., Mannhaupt, G., Mauceli, E., Mewes, H. W., Mitterbauer, R., Muehlbauer, G., Munsterkotter, M., Nelson, D., O'Donnell, K., Ouellet, T., Qi, W. H., Quesneville, H., Roncero, M. I. G., Seong, K. Y., Tetko, I. V., Urban, M., Waalwijk, C., Ward, T. J., Yao, J. Q., Birren, B. W., and Kistler, H. C. 2007. The *Fusarium graminearum* genome reveals a link between localized polymorphism and pathogen specialization. Science 317:1400-1402.

Cuzick, A., Urban, M., and Hammond-Kosack, K. 2008. *Fusarium graminearum* gene deletion mutants *map1* and *tri5* reveal similarities and differences in the pathogenicity requirements to cause disease on *Arabidopsis* and wheat floral tissue. New Phytol. 177:990-1000.

Desjardins, A. E., McCormick, S. P., and Appell, M. 2007. Structure-activity relationships of trichothecene toxins in an *Arabidopsis thaliana* leaf assay. J. Agric. Food Chem. 55:6487-6492.

Gale, L. R., Bryant, J. D., Calvo, S., Giese, H., Katan, T., O'Donnell, K., Suga, H., Taga, M., Usgaard, T. R., Ward, T. J., and Kistler, H. C. 2005. Chromosome complement of the fungal plant pathogen *Fusarium graminearum* based on genetic and physical mapping and cytological observations. Genetics 171:985-1001.

Gardiner, D. M., Kazan, K., and Manners, J. M. 2009. Novel genes of *Fusarium graminearum* that negatively regulate deoxynivalenol production and virulence. Mol. Plant-Microbe Interact. 22:1588-1600.

Gentleman, R. C., Carey, V. J., Bates, D. M., Bolstad, B., Dettling, M., Dudoit, S., Ellis, B., Gautier, L., Ge, Y. C., Gentry, J., Hornik, K., Hothorn, T., Huber, W., Iacus, S., Irizarry, R., Leisch, F., Li, C., Maechler, M., Rossini, A. J., Sawitzki, G., Smith, C., Smyth, G., Tierney, L., Yang, J. Y. H., and Zhang, J. H. 2004. Bioconductor: Open software development for computational biology and bioinformatics. Genome Biol. 5:R80.

Gerton, J. L., DeRisi, J., Shroff, R., Lichten, M., Brown, P. O., and Petes, T. D. 2000. Global mapping of meiotic recombination hotspots and coldspots in the yeast *Saccharomyces cerevisiae*. Proc. Natl. Acad. Sci. U.S.A. 97:11383-11390.

Güldener, U., Seong, K.-Y., Boddu, J., Cho, S., Trail, F., Xu, J.-R., Adam, G., Mewes, H.-W., Muehlbauer, G. J., and Kistler, H. C. 2006. Development of a *Fusarium graminearum* Affymetrix GeneChip for profiling fungal gene expression in vitro and in planta. Fungal Genet. Biol. 43:316-325

Guenther, J. C., and Trail, F. 2005. The development and differentiation of *Gibberella zeae* (anamorph: *Fusarium graminearum*) during colonization of wheat. Mycologia 97:229-237.

Hallen, H. E., and Trail, F. 2008. The L-type calcium ion channel Cch1 affects ascospore discharge and mycelial growth in the filamentous fungus *Gibberella zeae* (anamorph *Fusarium graminearum*). Eukaryot. Cell 7:415-424.

Hallen, H. E., Huebner, M., Shiu, S. H., Güldener, U., and Trail, F. 2007. Gene expression shifts during perithecium development in *Gibberella zeae* (anamorph *Fusarium graminearum*), with particular emphasis on ion transport proteins. Fungal Genet. Biol. 44:1146-1156.

Hou, Z. M., Xue, C. Y., Peng, Y. L., Katan, T., Kistler, H. C., and Xu, J. R. 2002. A mitogen-activated protein kinase gene (*MGV1*) in *Fusarium graminearum* is required for female fertility, heterokaryon formation, and plant infection. Mol. Plant-Microbe Interact. 15:1119-1127.

Irizarry, R. A., Bolstad, B. M., Collin, F., Cope, L. M., Hobbs, B., and Speed, T. P. 2003a. Summaries of Affymetrix GeneChip probe level data. Nucleic Acids Res. 31:e15.

Irizarry, R. A., Hobbs, B., Collin, F., Beazer-Barclay, Y. D., Antonellis, K. J., Scherf, U., and Speed, T. P. 2003b. Exploration, normalization, and summaries of high density oligonucleotide array probe level data. Biostatistics 4:249-264.

Jansen, C., von Wettstein, D., Schafer, W., Kogel, K. H., Felk, A., and Maier, F. J. 2005. Infection patterns in barley and wheat spikes inoculated with wild-type and trichodiene synthase gene disrupted *Fusarium graminearum*. Proc. Natl. Acad. Sci. U.S.A. 102:16892-16897.

Keogh, R. C., Deverall, B. J., and McLeod, S. 1980. Comparison of histological and physiological responses to *Phakopsora pachyrhizi* in resistant and susceptible soybean. Trans. Br. Mycol. Soc. 74:329-333.

Kimura, M., Tokai, T., Takahashi-Ando, N., Ohsato, S., and Fujimura, M.

2007. Molecular and genetic studies of *Fusarium* trichothecene biosynthesis: Pathways, genes, and evolution. Biosci. Biotechnol. Biochem. 71:2105-2123.

Kistler, H. C., and Benny, U. 1992. Autonomously replicating plasmids and chromosome rearrangement during transformation of *Nectria haematococca*. Gene 117:81-89.

Kuspa, A., and Loomis, W. F. 1992. Tagging developmental genes in *Dictyostelium* by restriction enzyme-mediated integration of plasmid DNA. Genetics 89:8803-8807.

Lee, S. E., and Myung, K. 2009. Faithful after break-up: Suppression of chromosomal translocations. Cell. Mol. Life Sci. 66:3149-3160.

McCormick, S. P., Harris, L. J., Alexander, N. J., Ouellet, T., Saparno, A., Allard, S., and Desjardins, A. E. 2004. Tri1 in *Fusarium graminearum* encodes a P450 oxygenase. Appl. Environ. Microbiol. 70:2044-2051.

Nierman, W. C., Pain, A., Anderson, M. J., Wortman, J. R., Kim, H. S., Arroyo, J., Berriman, M., Abe, K., Archer, D. B., Bermejo, C., Bennett, J., Bowyer, P., Chen, D., Collins, M., Coulsen, R., Davies, R., Dyer, P. S., Farman, M., Fedorova, N., Feldblyum, T. V., Fischer, R., Fosker, N., Fraser, A., Garcia, J. L., Garcia, M. J., Goble, A., Goldman, G. H., Gomi, K., Griffith-Jones, S., Gwilliam, R., Haas, B., Haas, H., Harris, D., Horiuchi, H., Huang, J., Humphray, S., Jimenez, J., Keller, N., Khouri, H., Kitamoto, K., Kobayashi, T., Konzack, S., Kulkarni, R., Kumagai, T., Lafton, A., Latge, J. P., Li, W. X., Lord, A., Majoros, W. H., May, G. S., Miller, B. L., Mohamoud, Y., Molina, M., Monod, M., Mouyna, I., Mulligan, S., Murphy, L., O'Neil, S., Paulsen, I., Penalva, M. A., Pertea, M., Price, C., Pritchard, B. L., Quail, M. A., Rabbinowitsch, E., Rawlins, N., Rajandream, M. A., Reichard, U., Renauld, H., Robson, G. D., de Cordoba, S. R., Rodriguez-Pena, J. M., Ronning, C. M., Rutter, S., Salzberg, S. L., Sanchez, M., Sanchez-Ferrero, J. C., Saunders, D., Seeger, K., Squares, R., Squares, S., Takeuchi, M., Tekaia, F., Turner, G., de Aldana, C. R. V., Weidman, J., White, O., Woodward, J., Yu, J. H., Fraser, C., Galagan, J. E., Asai, K., Machida, M., Hall, N., Barrell, B., and Denning, D. W. 2005. Genomic sequence of the pathogenic and allergenic filamentous fungus *Aspergillus fumigatus*. Nature 438:1151-1156.

Ochiai, N., Tokai, T., Nishiuchi, T., Takahashi-Ando, N., Fujimura, M., and Kimura, M. 2007. Involvement of the osmosensor histidine kinase and osmotic stress-activated protein kinases in the regulation of secondary metabolism in *Fusarium graminearum*. Biochem. Biophys. Res. Commun. 363:639-644.

O'Donnell, K., Kistler, H. C., Tacke, B. K., and Casper, H. H. 2000. Gene genealogies reveal global phylogeographic structure and reproductive isolation among lineages of *Fusarium graminearum*, the fungus causing wheat scab. Proc. Natl. Acad. Sci. U.S.A. 97:7905-7910.

Parry, D. W., Jenkinson, P., and McLeod, L. 1995. Fusarium ear blight (scab) in small-grain cereals—a review. Plant Pathol. 44:207-238.

Powell, W. A., and Kistler, H. C. 1990. In vivo rearrangement of foreign DNA by *Fusarium oxysporum* produces linear self-replicating plasmids. J. Bacteriol. 172:3163-3171.

Proctor, R. H., Hohn, T. M., and McCormick, S. P. 1995. Reduced virulence of *Gibberella zeae* caused by disruption of a trichothecene toxin biosynthetic gene. Mol. Plant-Microbe Interact. 8:593-601.

Ramamoorthy, V., Zhao, X. H., Snyder, A. K., Xu, J. R., and Shah, D. M. 2007. Two mitogen-activated protein kinase signalling cascades mediate basal resistance to antifungal plant defensins in *Fusarium graminearum*. Cell. Microbiol. 9:1491-1506.

R Development Core Team. 2006. R: A Language and Environment for Statistical Computing. R Foundation for Statistical Computing, Vienna.

Redman, R. S., and Rodriguez, R. J. 1994. Factors affecting the efficient transformation of *Colletotrichum* species. Exp. Mycol. 18:230-246.

Ruepp, A., Zollner, A., Maier, D., Albermann, K., Hani, J., Mokrejs, M., Tetko, I., Güldener, U., Mannhaupt, G., Munsterkotter, M., and Mewes, H. W. 2004. The FunCat, a functional annotation scheme for systematic classification of proteins from whole genomes. Nucleic Acids Res. 32:5539-5545.

Sambrook, J., Fritsch, E., and Maniatis, T. 1989. Molecular Cloning: A Laboratory Manual. Cold Spring Harbor Laboratory Press, Plainview, NY, U.S.A.

Seong, K. Y., Pasquali, M., Zhou, X. Y., Song, J., Hilburn, K., McCormick, S., Dong, Y. H., Xu, J. R., and Kistler, H. C. 2009. Global gene regulation by *Fusarium* transcription factors Tri6 and Tri10 reveals adaptations for toxin biosynthesis. Mol. Microbiol. 72:354-367.

Smyth, G. K. 2005. Limma: Linear models for microarray data. In: Bioinformatica and Computational Biology Solutions Using R and Bioconductor. R. Gentleman, V. Carey, S. Dudoit, R. Irizarry, and W. Huber, eds. Springer, New York.

Trail, F. 2009. For blighted waves of grain: *Fusarium graminearum* in the postgenomics era. Plant Physiol. 149:103-110.

Trail, F., and Common, R. 2000. Perithecial development by *Gibberella zeae*: A light microscopy study. Mycologia 92:130-138.

Trail, F., Xu, J. R., San Miguel, P., Halgren, R. G., and Kistler, H. C. 2003. Analysis of expressed sequence tags from *Gibberella zeae*. (anamorph *Fusarium graminearum*). Fungal Genet. Biol. 38:187-197.

Turgeon, B. G., Garber, R. C., and Yoder, O. C. 1987. Development of a fungal transformation system based on selection of sequences with promoter activity. Mol. Cell. Biol. 7:3297-3305.

Urban, M., Mott, E., Farley, T., and Hammond-Kosack, K. 2003. The *Fusarium graminearum MAP1* gene is essential for pathogenicity and development of perithecia. Mol. Plant Pathol. 4:347-359.

Winnenburg, R., Urban, M., Beacham, A., Baldwin, T. K., Holland, S., Lindeberg, M., Hansen, H., Rawlings, C., Hammond-Kosack, K. E., and Kohler, J. 2008. PHI-base update: Additions to the pathogen-host interaction database. Nucleic Acids Res. 36:D572-D576.

AUTHOR-RECOMMENDED INTERNET RESOURCES

OmniMapFree software: www.omnimapfree.org
The Plant Expression database (PLEXdb): www.plexdb.org